AD-A069 669 SOUTHERN UNIV BATON ROUGE LA DEPT OF MECHANICAL ENGI--ETC F/G 11/6
AN INVESTIGATION OF MECHANISMS EFFECTING ENVIRONMENTAL STRESS C--ETC(U)
JAN 79 I J GRAHAM N00019-78-C-0065

UNCLASSIFIED NL

| OF |
AD A069669

END
DATE FILMED
7-79
DDC

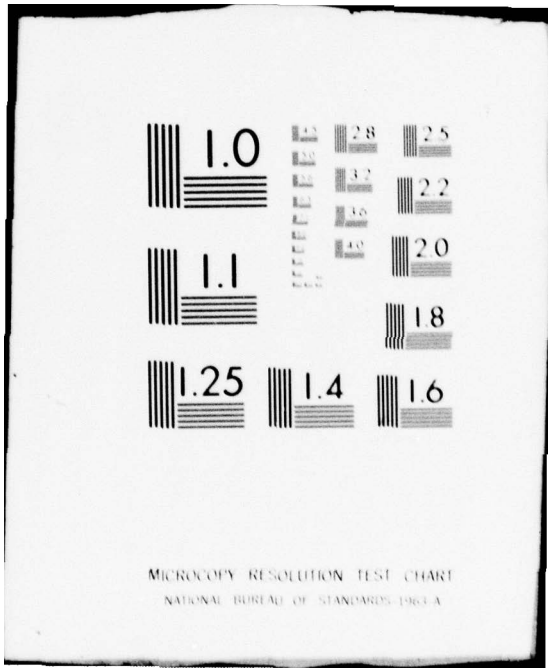
1.0
1.1
1.25
1.4
1.6
2.8
3.2
3.6
4.0
2.5
2.2
2.0
1.8
MICROCOPY RESOLUTION TEST CHART
NATIONAL BUREAU OF STANDARDS-1963-A

LEVEL II

12

"AN INVESTIGATION OF MECHANISMS EFFECTING ENVIRONMENTAL STRESS CRACKING IN TITANIUM ALLOY"

January 20, 1979

Work Performed Under The Direction of
Ira J. Graham
(Principal Investigator)

Mechanical Engineering Department
Southern University
Baton Rouge, Louisiana 70813

Under The Direction of Navair Scientific Officer:

T. F. Kearns
Naval Air Systems
Command
Department of the Navy
Washington, D.C. 20361

H11 211

Southern Univ., Baton Rouge, LA
Dept. of Mechanical Engineering

12

6

AN INVESTIGATION OF MECHANISMS EFFECTING ENVIRONMENTAL STRESS CRACKING IN TITANIUM ALLOY.

11 20 Jan[redacted] 79 — 12 24p.

Work Performed Under The Direction of
10 Ira J. Graham
(Principal Investigator)

Mechanical Engineering Department
Southern University
Baton Rouge, Louisiana 70813

Under The Direction of Navair Scientific Officer:

T. F. Kearns
Naval Air Systems
Command
Department of the Navy
Washington, D.C. 20361

15
Contract No. N00019-78-C-0065

411911

ACKNOWLEDGEMENT

The investigation period involved the efforts of five upper level Mechanical Engineering students, two senior level Business students, the faculty alternate and myself. The writer wishes to express appreciation and thanks for the interest and effort given by Messers Freddie McFarland, David Emanuel, Alaric Buckner, Miss Joann Taylor, all senior Mechanical Engineering majors, and Miss Patti Cade, a junior Mechanical Engineering student. Also thank goes to Dr. John Tabony for his assistance as the faculty alternate on the project. Appreciation and thanks is also extended to Dr. Dale Moyen and Dr. Cedric Beacham of the Naval Research Laboratory for their encouraging remarks and assistance in obtaining some good reference literature.

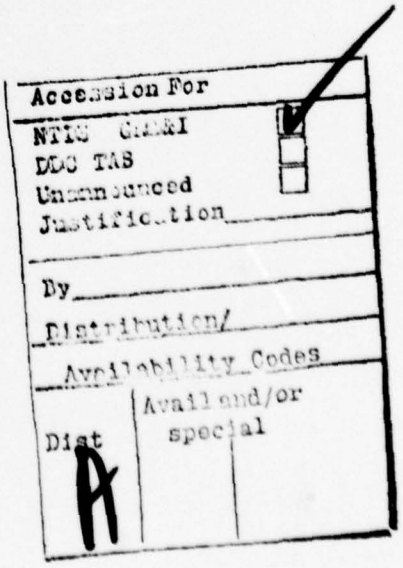

Table of Content

"AN INVESTIGATION OF MECHANISMS EFFECTING ENVIRONMENTAL STRESS CRACKING IN TITANIUM ALLOYS"

Abstract:

The Acoustic Emission System has been able to detect and record crack growth in a titanium alloy (Ti6Al4V) under a less than critical stress intensity (K_1) in a methanol environment. The fracture mechanics concept was applied to the data obtained on the 25.4mm (1 inch) modified wedge-open-load (WOL) specimen with a constant-open-displacement (COD) crack. A closed-loop environment system contained the specimen, methanol and piezoelectric transducer for the duration of the crack propagation under the sustained load. The crack growth to cumulative emissions count (da/dn) shows a decreasing linear relationship to the stress intensity (K_1).

Introduction:

Titanium alloys exhibit several specific properties that make their use very desirable in the hydrospace and aerospace structures. Titanium 6Al4V alloy has exhibited susceptibility to environmental attack under sustained loads and crack propagation occurs which has ultimately caused failure in the structure even at a sub-critical stress intensity level.

The alpha-beta titanium alloy (Ti6Al4V) used in this investigation was machined into bolt loading type WOL test specimens from the specifications given in the ASTM-E-399-74 standard, with an increase in the depth of the specimen (W). Nine specimens were solution heat treated at 914C (1678F)

under a dry grade nitrogen atmosphere for two hours. The nitgrogen was released into the electric arc furnace chamber at 3.5 cubic feet per hour, providing an oxygen free environment. A rapid oil quench was used. A thin film averaging one mil thick had to be removed from the specimens before testing. The dry grade nitrogen was used to purge the closed-loop environment test chamber before the specimens were inserted and during the sustained load environment attack.

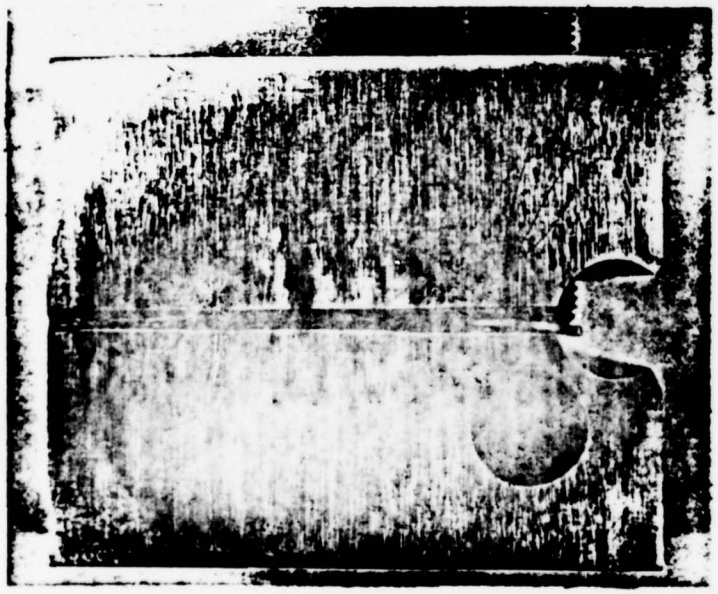

Figure 1. The 25.4mm WOL test specimen machined in the Mechanical Engineering laboratory. The knife edges on the semi-circle were cut to hold the MTS clip gage for load calibration. The thin copper sheet was inserted between the steel bolt and titanium alloy to reduce galling effect. The environmental crack was seen moving in the groove for 3.4 mm (0.134 in) then suddenly moving at a sharp angle to the groove and later growing back into the groove.

The fatigue load calibration compliance required to pre-crack the test specimen was determined by the fracture mechanics equation $\Delta P = \Delta K(B)\ (\sqrt{W})/f(a/W)$[1], where a = crack length, ΔK = 15 psi $\sqrt{in}$, and W = depth of specimen and f/(a/w) = 12.2. Pre-cracks were between 0.80 and 0.95mm (0.022 and 0.037in) at 50 Hz fatigue cycle.

Figure 2. The sustained loaded test specimen can be seen in the closed-loop environment chamber. The nitrogen, methanol, drive line to the AE system, and therometer were passed through the top cap of the chamber tube. The micrometer traveling microscope follows and measures the crack length.

The sustained load calibration was calculated in terms of a stress intensity factor (K_1) by the equation,

$$K_1 = (P/(B_n)\sqrt{W})[29.6(a/w)^{1/2} - 185.5(a/W)^{3/2} + 655.7\ (a/W)^{5/2} - 1017(a/W)^{7/2} + 638.9(a/W)^{9/2}],$$

where a = crack length, W = depth of specimen, B_n = thickness across grooves, and P = applied load.[2]

The acoustic emission system received the crack output data

through the piezoelectric tranducer amplified to 85dB and band-pass filtered in a frequency range of 100 to 300 kHz. This data were fed into a digital counter set to sum all incoming signals (accumulation mode) and displayed on the y-axis of the x-y plotter. Macrocracks in the order of 0.87mm to 1.77mm (.035 in to .068 in) were measured through the Gaertner traveling microscope to correspond to some acoustic signals recorded on the x-y plotter.

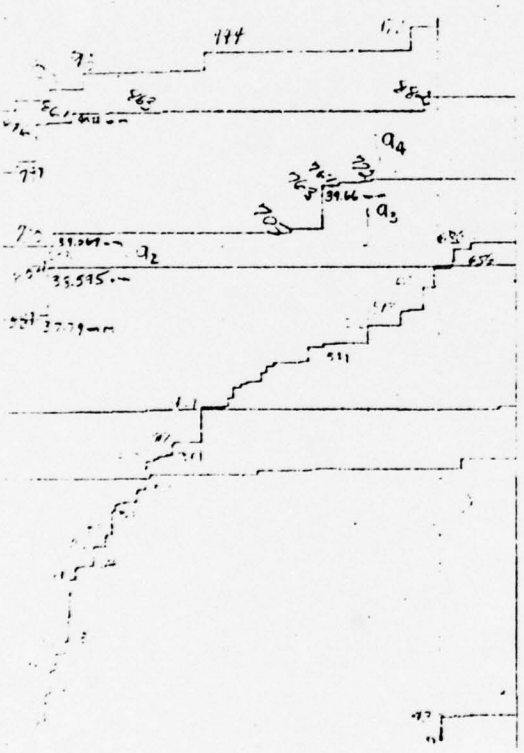

Figure 3. The cumulative emission counts coming off the specimen under environment attack and recorded on the y-axis of the x-y plotter. The burst-type emission is similar throughout the specimens tested. Crack growth length was marked to correspond to the emission amplitude where possible.

All specimens were pulled apart after the environment chamber test and the fractured surfaces were examined under a 30X magnification. The macro-structure revealed additional cracks within the structure as well as the formation of small island like crystals that could not be observed by the traveling microscope.

Figure 4. Another specimen under test revealed the same burst-type emissions. The emission count rate is faster for the first two to three minutes then grows constant while the amplitude of the burst are generally constant.

Eight sections were cut from four different test specimens and microstructures were prepared for examinations. Kroll's reagent was used as the etchant. The microstructure revealed the acicular type (Widmanstatten structure) througout the

several specimens. The typical environmentally influenced crack structure is seen in Figure 5.

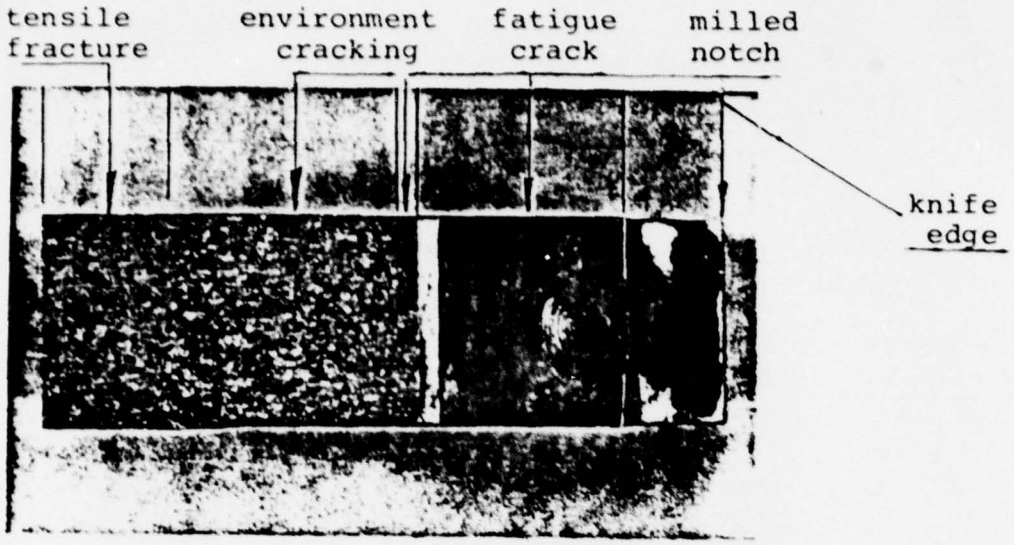

Figure 5. The test specimen separated after the environment test and several hours in the dessicator. The knife edge for clip gage #1, the machined notch zone #2, the fatigure crack zone #3, the sustained load environment attack zone #4, and the tensile fracture zone #5 are shown.

Materials and Procedure:

The 25.4mm (1.00 in) WOL test specimen was designed to the ASTM-E-399-74 specifications. The depth of the specimen (W) was increased to 67.47mm (2.665 in) to allow more crack growth in the environment and maintain a plane strain mode. These were machined from the as received annealed titanium 6Al4V alloy with the depth of the specimen (W) in the rolled directions, Figure 1. These were heat treated at 914C (1674F) for two hours in a dry grade introgen atmosphere flowing into the electric arc furnace at 3.5 cubic feet per hour and oil quenched to room temperature, 26C (78F). They were then reheated to 749C (1380F) into the beta anneal range for two hours. The furnace was shut down and the specimens furnaced

cooled to 535C (1000F) then cooled in the laboratory atmosphere to 26C (78F).

All the specimens were descaled by mechanical means using 50, 80, and 120 grit silicon carbide abrasive belts. The side grooves designed to guide the crack movement were hand finished with 240 grit. The specimen were then placed in a clean dry dessicator. Pre-cracking was done on the electronic servo-hydraulic dynamic test machine. Each specimen was given the pre-crack by the calculated load calibration and then the initial stress intensity (K_1) was applied as the sustained load by use of the digital multimeter, MTS clip gage and bolt and wrench. The initial stress intensity factor (K_1) (9.85 MPa $\sqrt{mm}$) was at approximately two-thirds the critical stress (K_{1c}), the stress level below which crack growth does not occur in the laboratory atmosphere. Under this load condition, each specimen was placed into the environment test chamber. The piezoelectric transducer was fastened to the specimen with a viscous resin and the drive line fastened by BNC connectors to the Model 3000 Acoustic Emission System, on to which the x-y recorder is attached, Figure 2. The Gaertner traveling microscope, 32X magnification, was set up to optically follow the crack growth in the specimen for the test period.

During a period of ten to twelve hours in the test environment, the crack growth measurements were recorded optically and where possible these were recorded on the y-axis plot to correspond

to the amplitude of the cumulative emission (dn) recorded on the plotter. At crack arrest, the specimens were removed from the test system and the viscous resin removed. They were then wrapped in absorbant paper towel and stored in the dry dessicator for observation before pulling part.

The entire macrostructure of the test specimen was examined through the stereomicroscope at 32X magnification. Sharp contrast was observed in both the color and nature of the fracture produced by the environment attack under sustained load and by that the tensile fracture, Figure 5. The fracture toughness equation, $K_1 = (P_1/B_n W^{1/2})[29.6(a/w)^{1/2} - 185.5(a/w)^{3/2} + 655.5(a/w)^{5/2} - 1017.0(a/w)^{7/2} + 638.9(a/w)^{9/2}]$ was used to determine the stress intensity at several measured crack lengths in the area under environment attack.

Discussion:

The 25.4mm WOL specimen under the sustained bolt load maintained a constant-open-displacement (COD), in a plane strain mode and proved adequate in differeniating between crack growth caused by environment attack and that due to the critical stress intensity 7178 psi $\sqrt{in}$ (K_1c) in the laboratory atmosphere. No crack growth was seen optically in the specimens that were given calculated stress intensities between 6000-6900 psi $\sqrt{in}$ while they were in the laboratory atmosphere or in the dessicator. Acoustic signals were detected and recorded on the x-y plotter within a few seconds after these same specimens came in contact with the methanol in the closed-loop environment

test chamber, Figure 4. After the crack arrested in specimen (A) under the stress intensity 6936 psi $\sqrt{in}$ (K_1) in the menthanol test environment, it was removed and stressed to 7178 psi $\sqrt{in}$ (K_1). Under this higher stress intensity no visual crack growth was observed optically in the specimen in the laboratory atmosphere. This specimen was returned to the mehtanol test environment in the closed-loop test chamber system and the crack growth was detected optically and through the AE system. The crack growth at this low stress intensity appears to be a result of a diffusion mechanism related to the methanol concentration, grain boundaries, and impurities at a crack tip stress intensity. Further investigation shall be directed on this phenomenum.

The acoustic signals output at the piezoelectric transducer was amplified to 85dB, filtered for frequencies between 100 and 300 kHz. The output was sent to a signal conditioner, digital counter, and summed as total cumulative acoustic signals (dn) for each burst-type crack and recorded on the y-axis. A ramp generator provided that full scale horizontal sweep on a 30 minute time base. The digital/analog accumulations were recorded as voltage output on the y-axis. The amplitude of the cumulative counts (ΣN) displayed, illustrated the effect of the environment in producing the burst-type crack movement, Figure 3. The crack length was measured along the groove of the specimen optically and recorded on the amplitude output of this signal at the x-y plotter. This was not possible at

all burst, even though the acoustic signals were constantly being received, an indication that the crack was still moving. The crack movement was observed to move slower by an order of magnitude in the beta annealed specimen than in the as received mill annealed. There was no pronounced leading edge in the crack, but the crack did appear to move from inside to out. This would account for the burst-type emissions, but no observed crack growth for the events.

Examinations of the fractured surface under the stereo-microscope at 32X magnification revealed small crystalline particles held by a thin boundary in the shear cavities throughout the environment attacked zone of the beta annealed specimens, Figure 7. The angular directions of the shear cavities with the horizontal crack movement appear to illustrate the anisotropic behavior in the crack movement. The length of the cavities tend toward the direction of the major crack movement; however, these cavities showed depths up to half their length with additional shear cracking at the base. The small crystals measured up to 0.15mm (.006 in) thick and as much as two times this in length. Other investigaters have observed this phenomenum in the beta-annealed titanium alloy. This bifurcation effect probably reduced the stress intensity and accounted for the high amplitude cumulative counts (ΣN) recorded on the y-axis of the plotter. The scanning beam electron microscope should provide additional information on this phenomenum.

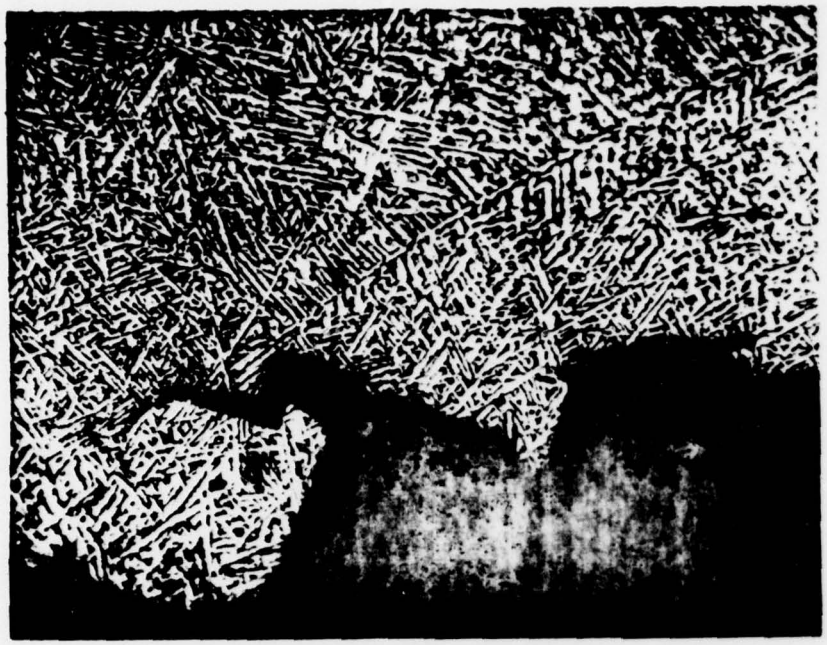

Figure 7. Transgranular cracking is seen along the crack edge of the microstructure of acicular alpha (light) and aged beta. The continuous acicular alpha boundaries (transformed beta) is shown.

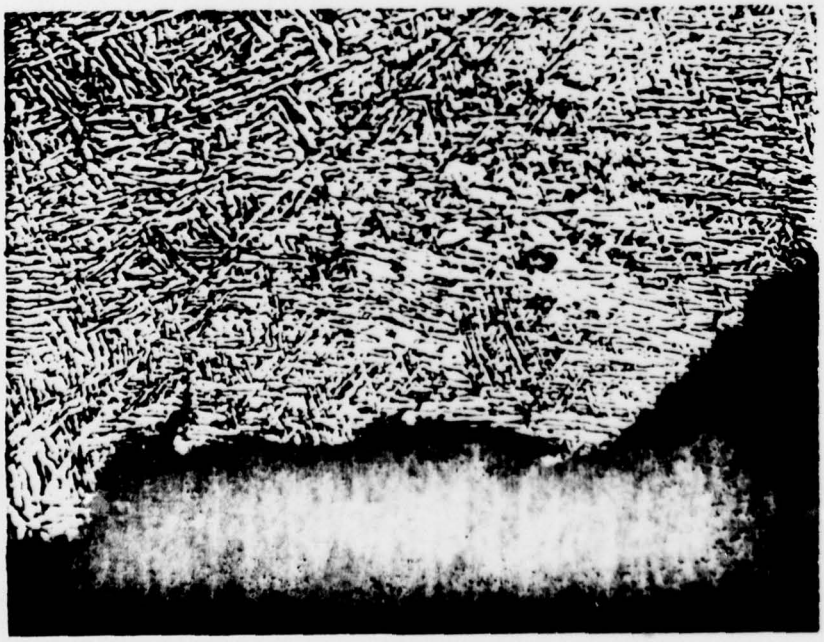

Figure 8. The photomicrograph of the beta annealed fracture reveals transgranular cracking at the edge of the crack propagation boundary. A continuous acicular alpha boundary stretches across the matrix. Primary alpha (light) is seen in the lower right.

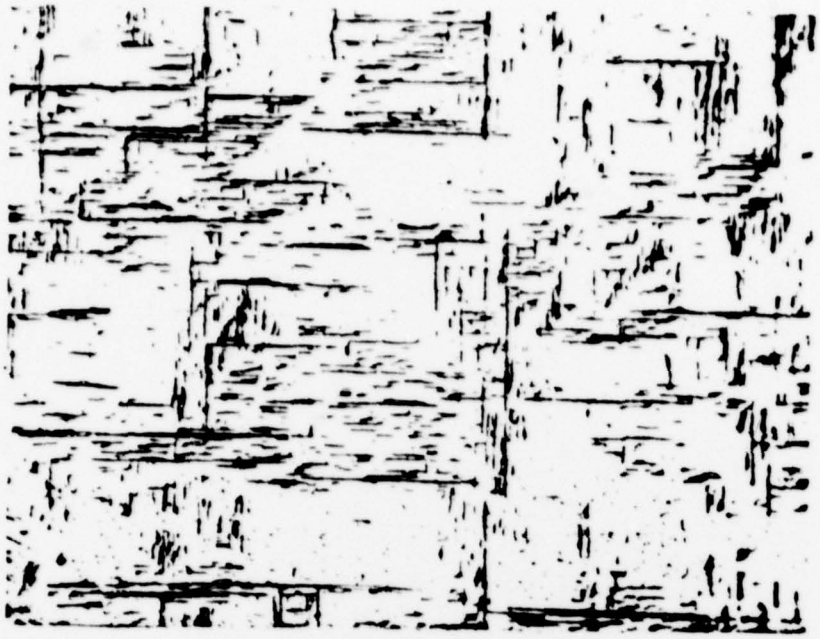

Figure 9. Wide plates of acicular alpha (transformed beta) and thin plates of transformed beta was found in the microstructure of test specimen (D).

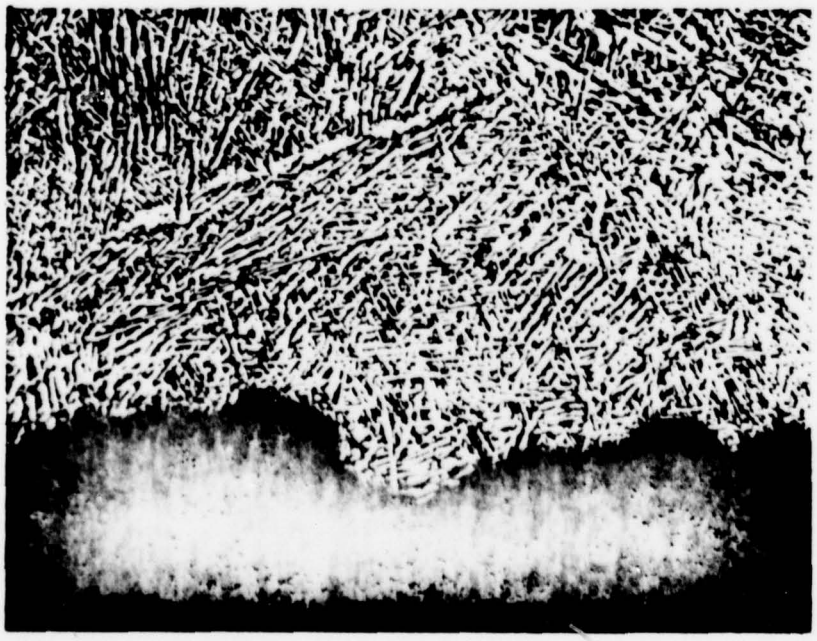

Figure 10. The photomicrograph shows fine acicular alpha with aged beta. A course acicular alpha boundary (light) is highly visible. The light gray boundary along the crack edge results from the methanol environment attack.

The crack growth was more rapid and extended over a longer period in the as received mill annealed specimen than in the beta annealed specimen. The data shown in Figure 12 indicates that the beta annealed specimens shows a decrease in strength and ductility when compared with the as received mill annealed specimen. Specimen (A) was environmentally tested under a lower and higher sustained load. The stress intensity increased by 30% but the slope of the stress intensity curve remains constant.

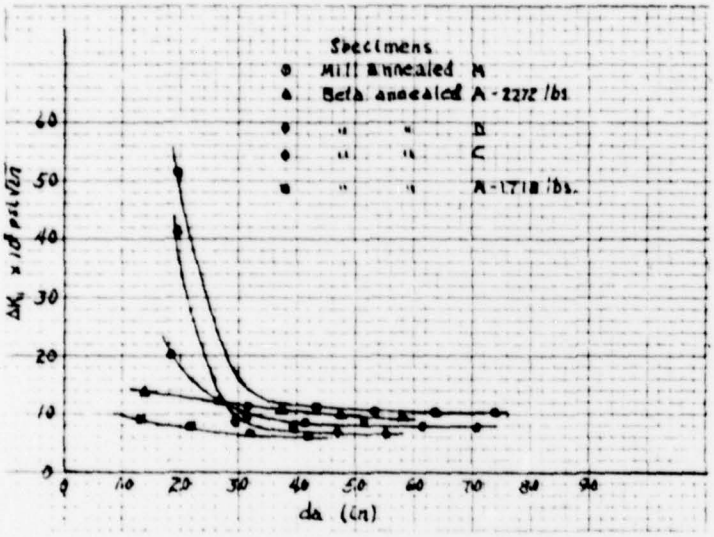

Figure 11. The data shows a comparism of the environment (methanol) induced crack growth in the test specimens under sustained bolt load conditions. Specimen (A) shows a curve for two different sustained load, but the slope of the curve remain constant.

This data is based on an observation that crack growth in the sustain loaded specimen was not observed to occur until the specimens was in contact with the methanol. The crack growth was very active in the initial contact period, after the first hour the crack growth becomes less active. However,

some observations have seen rapid acoustic signals of high amplitude cracks recorded after crack arrest for 4 to 5 hours, Figure 4.

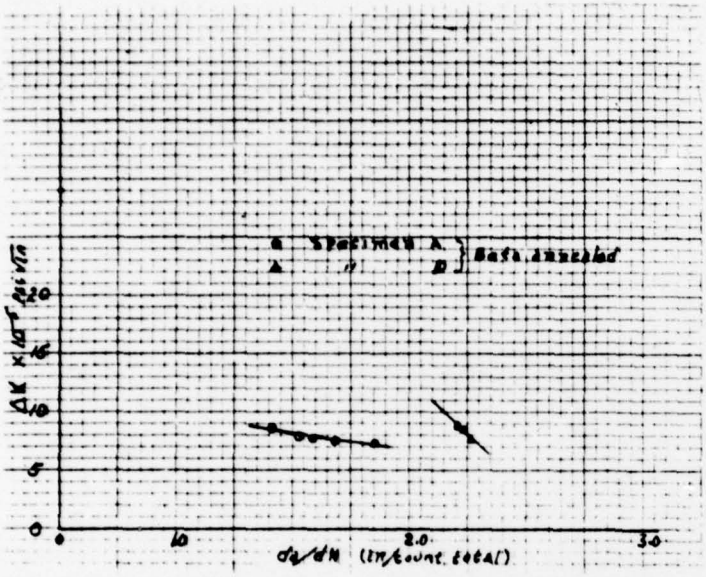

Figure 12. The stress intensity ΔK_I shows a linear decrease as the crack extends over the environment attack period.

The data shown in Figure 13, attempts to relate a ratio of cumulative emission counts to a specific crack burst to stress intensity seen by the specimen at that instant crack. More work shall be directed at this technique. The stress intensity tend to decrease linear with the extending crack and cumulative emission counts.

The heat treated specimens were descaled by a surface grinder and abrasive belts of #50, 80, and 120 grits. This operation did not improve the surface texture or hardness. A superficial surface hardness tester was not available to make this type surface hardness test.

Conclusion:

The closed-loop controlled environment isolated the low stressed test specimen from which acoustic signals were recorded in a frequency range of 100 - 300 kHz at a gain of 85dB. These signals were able to be identified as those resulting from crack propagation within the specimen. This suggest that crack growth resulting from environment effect may be detected and differeniated from other noise.

Data presented in the study shows that crack growth rate and length decreased significantly, approximately 32%, in the beta annealed specimens as compared to those of the as received mill annealed titanium 6Al4V. However, the Widmanstätten structure (acicular alpha) in the beta-annealed revealed a coarser grain microstructure and this resulted in decrease in ductility and strength.

The fractured macrostructure in the beta annealed Ti6Al4V revealed large shear cavities of depth up to 0.57mm (.022 in) sloping at angles of 18 to 20 degrees to the horizontal plane. A few of these cavities revealed crack growth continuing from the base of the cavities downward and perpendicular to the primary crack growth direction. This relates to anisotropic behavior in the beta annealed crack growth. This mechanism may have been a contributing factor in the high decrease in crack growth rate and length.

The low stress intensity factors between 6228 and 7178 psi

$\sqrt{in}$ (42.8 - 49.5 MPa $\sqrt{mm}$) did not produce crack growth in the test specimens under laboratory atmosphere or in the dessicator over observed periods of ten to fifteen hours of sustain load condition. However, the methanol environment of the closed-loop test chamber triggered a crack movement in the specimen within ten to fifteen seconds. Crack growth under this condition seems to be related to a diffusion mechanism which may involve methanol concentration, grain boundary energy and or impurities. Further effort will be directed in this area.

Problems:

The Acoustic Emission System is undergoing some updating in the sections that define the amplitude of the crack flow, quantify the acoustic signals, and measures the energy per emission event. This means about for to six weeks of down time in the application of the AE System in the investigation. A dry grade argon gas will be substituted for nitrogen gas as the cover gas for the specimen in the test and heat treatment.

REFERENCES

1. ASTM Standard Committee, A-24, Part 10, American Society for Testing Materials, Philadelphia, Pa., 1974.

2. ASTM Standard, E-399-74, Part 10, American Society for Testing Materials, Philadelphia, Pa., 1974, pp. 432-451.

3. "Enhancement of Fatigue Crack Growth and Fracture Resistance in Ti-6Al-4V and Ti-6Al-6V-25n Through Microstructural Modification", G.R. Yoder, L.A. Rooley, and T. W. Crooker, NRL Report 8049; Naval Research Laboratory: Washington, D.C., Nov. 24, 1976.

4. ASM, Atlas of Micostructures, American Society for Metals, Volume 7, Metal Park, Ohio, 1975

5. "Fatigue and Corrosion - Fatigue Crack Propogation in Intermediate - Strength Aluminum Alloys", T. W. Crooker, Paper no. 73, Naval Research Laboratory, Washington, D. C.

6. "Non-Destructive Characterization of Hydrogen Embrittlement Cracking By Acoustic Emission Techniques", H. L. Dunegan and A. S. Tetelman, Tech. Bual DRC-106 Dunegan/Endevco, San Juan Copistrano, California.

APPENDIX A

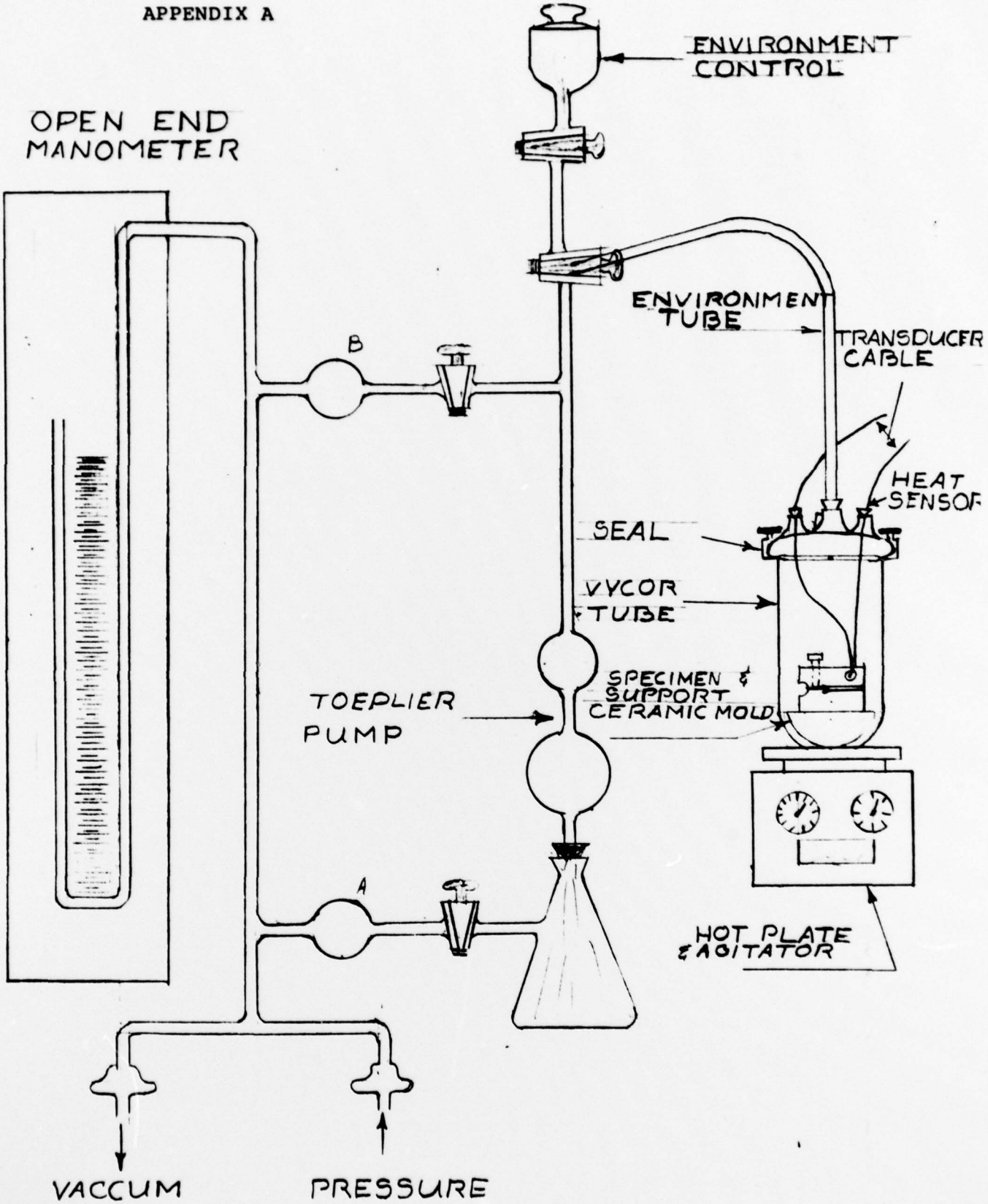

Fig. 12
Environment charging system. Specimen supports on a glazed ceramic mold without Vycortube.

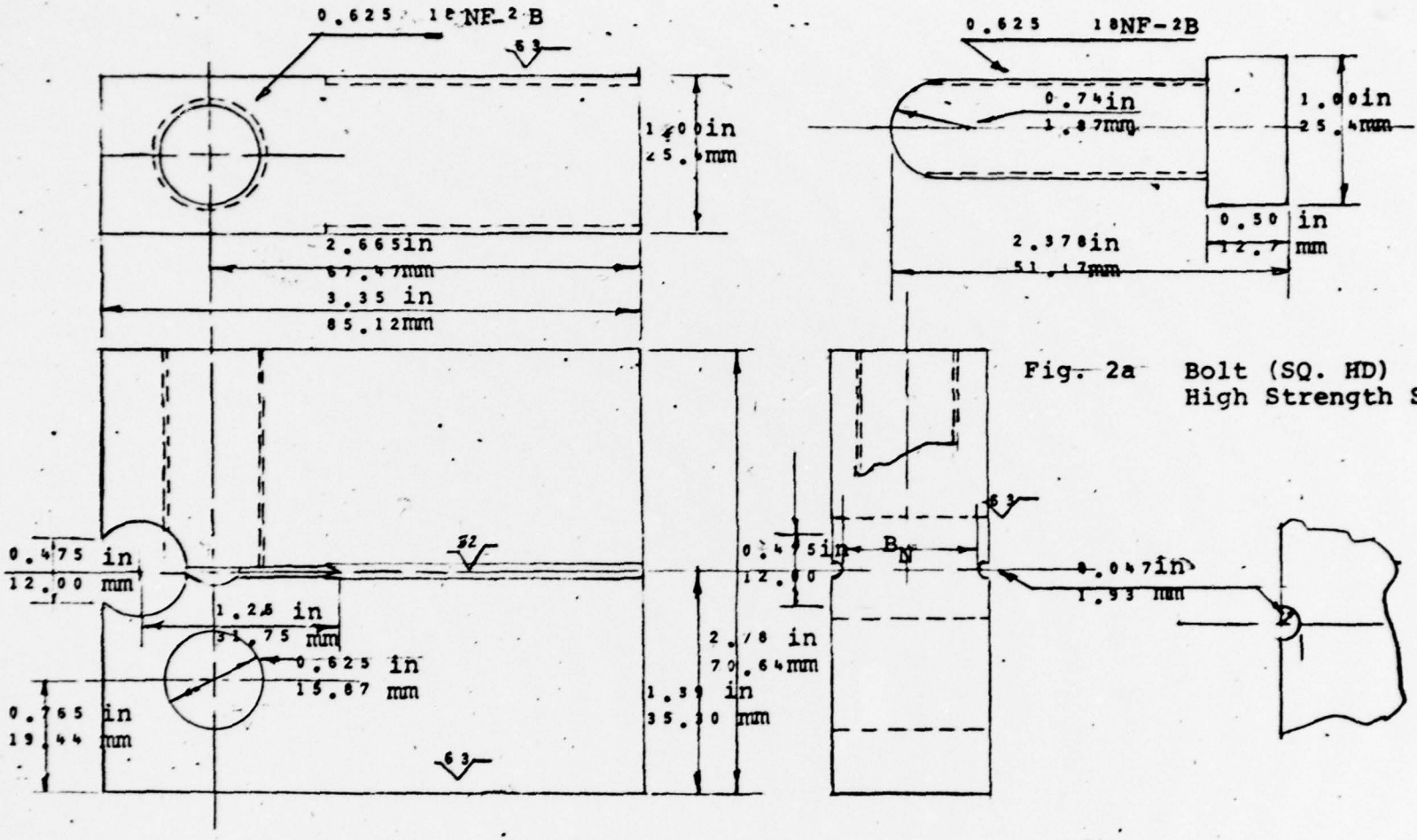

Fig. 2a Bolt (SQ. HD) High Strength Steel

Fig. 13 WOL (1T) Specimen (1 inch thick)